2016 IEEE/RSJ International Conference on Intelligent Robots and Systems (IROS)
Daejeon Convention Center
October 9-14, 2016, Daejeon, Korea

Morphological Design for Controlled Tensegrity Quadruped Locomotion

Dawn Hustig-Schultz[1], Vytas SunSpiral[2,4], and Mircea Teodorescu[1,3]

***Abstract*— From the viewpoint of evolution, vertebrates first accomplished locomotion via motion of the spine. Legs evolved later, to enhance mobility, but the spine remains central. Contrary to this, most robots have rigid torsos and rely primarily on movement of the legs for mobility. The force distributing properties of tensegrity structures presents a potential means of developing compliant spines for legged robots, with the goal of driving motion from the robots core. We present an initial exploration of the morphological design of a tensegrity quadruped robot, the first to the authors' knowledge, which we call MountainGoat, and its impact on controllable locomotion. All parts of the robot, including legs and spine, are compliant. Locomotion is aided by the use of central pattern generators, feedback control via a neural network, and machine learning techniques involving the Monte Carlo method as well as genetic evolution for parameter optimization. Control is demonstrated with three variations of MountainGoat, focusing on actuation of the spine as central to the locomotion process.**

I. INTRODUCTION

Current wheeled and rigid-bodied robots are limited in their mobility over rough terrains and in their ability to operate in unpredictable environments. This limits their usefulness for such tasks as space exploration, search and rescue missions, and missions in environments unsafe for humans. These environments are well suited for compliant quadruped robots.

Tensegrity structures, which originated in architecture as a disjoint set of compression members suspended in a system of continuous tension members, represents a more recently investigated solution to extending compliance to an entire robotic structure [1]. Tensegrity robots are lightweight and robust to failures, as the failure of one actuator leads to diminished performance rather than failure of performance. They are impact tolerant, as forces distribute evenly over the whole instead of being magnified into joints by internal lever arms, causing less damage to itself and to other objects in its environment.

Figure 1 shows a model of MountainGoat, a tensegrity quadruped robot based off an original model by Tom Flemons [2], balanced on a terrain filled with blocks. Of note in this figure is MountainGoat's passive terrain interaction, and how it naturally adapts to complex footing by utilizing the multiple degree-of-freedom compliance of its tensegrity spine. This ability of tensegrities to redistribute forces to achieve equilibrium is a compelling reason for their application to constructing robots that can traverse rugged ground. The goal of our research is to develop a quadruped robot with the agility and adaptability of a mountain goat.

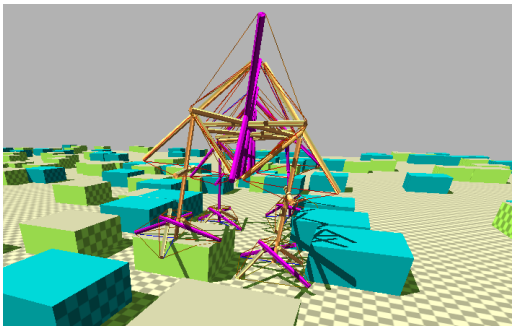

Fig. 1. The Quadruped balancing on blocks, naturally adapting to complex footing by utilizing the multi-DOF compliance of its tensegrity spine.

Prior studies with other tensegrity morphologies has shown robust locomotion over rough terrain [3], [4], [5], [6], [7], [8], [9], [10], [11]. The quadruped morphologies we present, however, have not yet been developed to the point where they can locomote over rugged ground. With the preliminary results presented here, we are beginning to understand the process of whole-body control, and how the spine provides support to shoulders and hips in order to lift legs. For instance, we have not quite achieved the amount of leg lift necessary to actively traverse rugged terrain. In addition, the control presented here is limited to spinal motions. Hence our quadruped has passive legs and still lacks knees, which enhance motion over obstacles. Nevertheless, our initial findings have given important insights toward our ultimate goal.

II. BACKGROUND

Boston Dynamics' BigDog and Spot robots have had success in navigating robust terrain including on ice and snow [12] [13]. These robots can be energy expensive, prone to single-point failures, and susceptible to damage on impact, to the robot itself as well as to objects and people in its environment. Degrave, et. al. have incorporated some compliance in the legs of quadruped robots [14]. These rigid bodied robots, however, represent more constrained solutions that lack the compliant spines that are central to the speed, agility, and stability of quadruped and biped locomotion [15].

The benefit of a compliant spine to quadruped locomotion has been studied by Zhao, et. al., simulating robots that have multiple spinal joints ranging in number from 1 to 12 [16]. Although improved locomotion was shown with two and four spinal joints, these simulated designs use one-DOF joints that

[1]University of California, Santa Cruz, Santa Cruz, CA 95064
[2]Authors with the NASA Ames Dynamic Tensegrity Robotics Lab, Moffett Field, CA 94035
[3]NASA-ARC Advanced Studies Laboratories, Moffett Field, CA 94035
[4]Stinger Ghaffarian Technologies, Greenbelt, MD 20770, USA

978-1-5090-3762-9/16/$31.00 ©2016 IEEE

represent single points of failure, and the legs of the robots in these simulations were completely rigid. Researchers at the University of Pennsylvania compared two robots with the same semi-rigid c-shaped legs, one with a rigid body and the other with a parallel elastic actuated spine. The robot with the elastic spine showed more distance and agility in forward leaps than its rigid bodied counterpart [17].

One of the earliest investigations of tensegrity locomotion involved gait production in a simple three-bar tensegrity structure by researchers at Cornell University [18]. Some robots, such as MITs Cheetah robot, have incorporated tensegrity principles in the legs, but not in the spine of the robot, where it could have greater benefit [19]. Although the legs of the Cheetah robot are very effective in forward motion, they are somewhat limited in the kind of lateral motion needed to give good balance and stability.

Researchers at the University of California, San Diego have studied the locomotion of a snake-like tensegrity structure for duct inspection [3], and Agogino, et. al. have studied locomotion of the SUPERBall bot, with the goal of exploring Saturn's moon Titan [4], [5]. Tensegrity structures can be used to model spines [20], and extensive research has been done by Mirletz, et. al. on flexible tensegrity spines for their potential benefit in locomotion, with the eventual goal of building compliant quadruped and biped robots [6], [7], [8], [9], [10], [11]. The study of tensegrity spines in these papers has demonstrated the robustness of tensegrity locomotion over rough terrain.

III. METHODS

Our structural design approach began with a fully passive model of MountainGoat, designed by Tom Flemons [2]. Due to the tendency of tensegrity structures to redistribute loads and deform to equilibrium shapes, designing for movement can be very counter intuitive, and structural design and control end up being highly coupled. Because of this property, many of our design iterations came about as a result of attempts to control previous model designs.

Inspired by evolution, and the central role spines play in vertebrate locomotion, we initially focused on driving motion from the spine. This approach allowed us to continue the research of Brian Mirletz [6], [7], [8], [9], [10], [11], by applying his tensegrity spine control research to MountainGoat. Thus, we use machine learning to optimize the controls for novel morphologies, allowing us to evaluate the effectiveness of a specific morphology.

The open source NASA Tensegrity Robotics Toolkit (NTRT) was used for simulation. NTRT is built on the Bullet Physics Engine, version 2.82, which handles rigid body dynamics to simulate the rods of the structure. This is supplemented by an additional custom soft body spring-cable model with contact dynamics, which is used to simulate the muscles of the structure. The dynamics of the spring-cable are based on Hooke's law for a linear spring, and collisions are detected using ghost objects within Bullet [9]. Internal cable and rigid body dynamics were previously validated within 1.3% error [21]. Additional tests validated steady state error on maximum cable tension within 6.1%, maximum system tension on hand-tuned controllers was validated within 7.9% error, and tensions from CPGs were validated within 1.6% error [9].

Simulations were run at 1000 Hz. Five different iterations of MountainGoat are presented. The stiffness, pretension, and damping parameters used for these models can be found in table I. For reference, a pretension setting of 700 is about 5N, 1000 is about 7N, 2500 is about 17.9N, and 3500 is about 25N. The last three of these model revisions were tested in simulation on flat terrain, using the actuation approach discussed below.

TABLE I
PARAMETERS USED FOR EACH MODEL

Model	Parts	pretension	stiffness	damping
Model 1: *Flemons*	All parts	700	2000	20
Model 2: *NewFeet*	All parts	700	2000	20
Model 3: *LongTorso*	Spine	0	1000	10
	Legs	2500	3000	30
	Feet	1000	1000	10
Model 4: *Spirals*	Spine	0	1000	10
	Legs	3500	4000	10
	Feet	1000	4000	10
Model 5: *NoFeet*	Spine	1000	2000	10
	Legs	3500	4000	10

A learning run starts with a Monte Carlo stage, where 30,000 random trials are generated. Each trial has a duration of 60 seconds and, since we use the distance traveled in one minute as the measure of fitness, this distance is determined by taking the difference between the location of the center of mass at the beginning and end of each trial. Those trials in which MountainGoat travels the greatest distance in any direction are considered the fittest trials. After the Monte Carlo stage ends, we evolve the fittest 40 trials via a genetic algorithm with crossover, mutation, and elitism. Given a complex parameter space with many peaks and valleys, we use Monte Carlo trials to find initial decent results, and then optimize them with the genetic algorithm. The mutation chance used was 50% while the mutation deviation was 3%.

Our approach to actuation reflects the hierarchical nature of biological nervous systems, with local reflexes at a lower level and Central Pattern Generators (CPGs) at a higher level [22]. Impedance control is used for the lower level reflexes, based on an equation first used for tensegrity by Orki, et. al. [23] and adapted to account for descending commands from the CPGs by Mirletz, et. al. [10]:

$$T = T_0 + K(L - L_0) + B(V - V_0) \quad (1)$$

T is the output tension, T_0 is the tension offset, and K is the position gain on the difference between the current length L and the desired length L_0. B is the velocity gain on the difference between the current velocity V and the desired trajectory V_0. This V_0 term is a descending command from the CPG.

The CPG equations used consist of adaptive phase coupled oscillator equations with frequency feedback [24], as well as amplitude and phase feedback [25], and were previously used by Mirletz, et. al. for locomotion of tensegrity spines [6]:

$$\dot{r}_i = \gamma(R_i + k_r F_r - r_i^2) r_i \tag{2.1}$$

$$\dot{\theta}_i = \omega_i + k_\theta F_\theta + \sum_j r_j w_{ij} sin(\theta_j - \theta_i - \phi_{ij}) \tag{2.2}$$

$$\dot{\omega}_i = k_\omega F_\omega \sin(\theta_i) \tag{2.3}$$

$$\dot{V}_i = r_i \cos(\theta_i) \tag{2.4}$$

where r_i is the wave's amplitude, ω_i is its frequency, and θ_i is its phase. V_i is the input to the impedance controller. The amplitude, as seen in equation 2.1, is set by the convergence parameter γ and the setpoint R_i. The phase, as seen in equation 2.2, is connected to neighboring nodes through the coupling weight w_{ij}, phase offset ϕ_{ij}, and the neighboring node's amplitude r_j. The constant terms k_r, k_θ, and k_ω are scalar gains on the corresponding feedback parameters F_r, F_θ, and F_ω. These feedback parameters come from outputs of an artificial neural network, and are used in a similar manner as in [25] and [6]. As in [6], this neural network consists of two input nodes for which the inputs are tension and length, one hidden layer of four nodes, and three output nodes for F_r, F_θ, and F_ω.

The CPG equations are integrated using ODEInt, which is part of the Boost C++ libraries [26]. Each actuator is coupled only to other actuators that share rigid bodies [6], [10]. Since our approach to control has up to this point focused on spine actuation, the linearity of the rigid bodies attached to these actuators ensures that there are at most three rigid bodies in each coupling set.

IV. RESULTS AND DISCUSSION

A. Mechanical Design

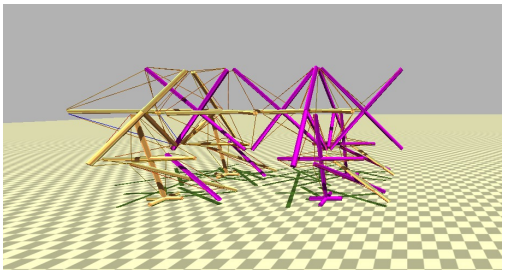

Fig. 2. Model 1 of the quadruped, *Flemons*, based off a design by Tom Flemons.

The initial design, *Flemons*, seen in figure 2, consists of a spine of six X-segments of four struts each, with three of the segments oriented vertically and three oriented horizontally. ten cables connect each segment in the spine, with the exception of the penultimate segment which is connected by fourteen cables. The hips and shoulders also consist of single T-segments, of three struts each. Each of the shoulders are connected to the spine by ten cables, and each of the hips are attached to the spine by nine cables. the hips connect to each other with one cable, to add stability. Legs also consisted of single X-segments, but with shorter support rods added to the bottom of each leg for stability. Each leg is connected to its corresponding hip or shoulder, foot, and spine by fourteen cables. The feet consist of two rods which cross each other, and 11 cables connecting these rods to the legs, for support. The full model has a total of 60 struts. In qualitative testing on hilly terrain, we found that the cross rods of the foot caught too easily on obstacles, and didn't provide enough stability to keep the structure standing.

Figure 3 shows *NewFeet*, which differs only in the feet. The bottom rod of the leg is extended by 5 cm, and a compliant foot, consisting of a four strut prism, replaces the two cross rods, and brings the model to a total of 68 struts. An extra muscle was also added to each hind leg, shown in red in figure 3, connecting these legs to the last vertebra in the spine to improve overall balance. This compliant foot provided more stability to the structure. In drop tests on hilly and block-filled terrains, these feet helped the model to maintain a standing position on landing, rarely falling over. *Flemons* and *NewFeet* were not actuated, but were primarily evaluated passively and qualitatively for structural stability.

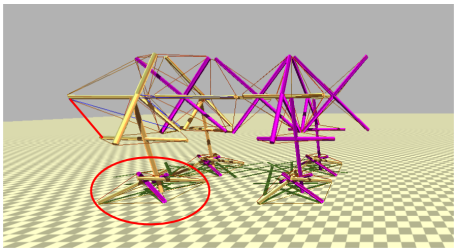

Fig. 3. The first revision of MountainGoat, *NewFeet* with improved compliant feet for better balance. Differences are shown in red.

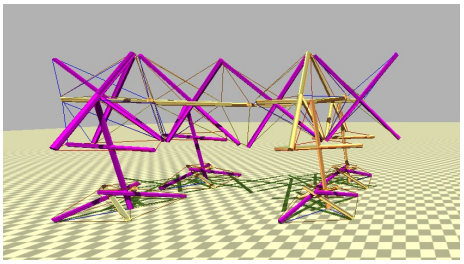

Fig. 4. The second revision of MountainGoat, *LongTorso*, with an extra vertebra added to the spine.

For ease of actuation, the structure was updated again by adding an extra vertebra to the spine, bringing the total number of struts to 52. This was done to simplify the initial approach to control, as each vertebra of the spine would have an equal number of CPGs. Then input parameters for only 8 CPGs on one vertebra would need to be learned, and then applied to the 7 identical spine segments, reducing the overall solution space. In comparison, *Flemons* and *NewFeet* would need to learn parameters for an additional 12 cables, to accommodate the penultimate vertebra. The change had

the extra benefit of adding a bit more torsion to the spine as well as to provide enough distance between the front and back feet to keep them from colliding with each other. Figure 4 shows this new model of MountainGoat, called *LongTorso*. LongTorso has a total of 56 CPGs, in the spine only, which actuate the simulated model. Results of spine actuation on this model can be seen in section IV-B.

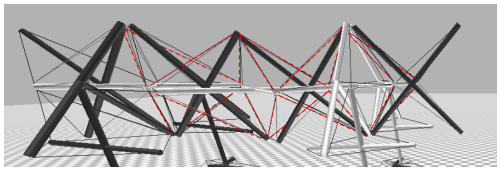

Fig. 5. A close-up of the spine on *Spirals*, showing the extra muscles added to the spine highlighted in red. Though these muscles appear almost as duplicates of the previously existing muscles, they only share one endpoint in common with each corresponding muscle from the original spine morphology.

As stated earlier, morphological design and actuation of a tensegrity robot are highly coupled, due to the tendency of these structures to redistribute loads and deform to equilibrium shapes. As an example, early attempts at manually designing a controller to lift a single leg resulted in the corresponding shoulder drooping toward the foot, rather than the leg lifting off the ground. Since the initial cable layout of the spine did not provide the stability to hold the shoulder up, two extra spirals of muscles were added to the spine, one clockwise and one counterclockwise. These extra twenty muscles, which serve a similar function as the latissimus dorsi muscles in many four-legged vertebrates, can be seen on *Spirals* in figure 5. The addition of these muscles helped increase torsion in the spine, which led to increased distance traveled in simulation, as is shown in section IV-B.

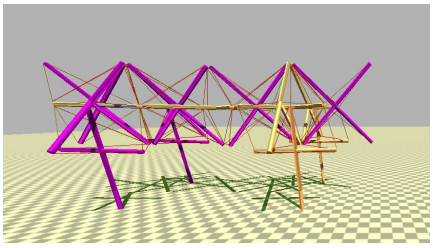

Fig. 6. Current model of MountainGoat, *NoFeet* with feet removed.

Simulations of control of the structures in figure 4 led to the conclusion that ground reaction force was being lost in the compliance of the feet. As shown on *NoFeet* in figure 6, the feet were thus removed, and two extra muscles were added between each leg and its adjacent body segment, to keep the model standing. This removal, which reduced the total amount of struts to 56, added more distance to simulations, as shown in section IV-B. *LongTorso*, *Spirals*, and *NoFeet* are 86 cm long by 42 cm wide by 36 cm tall. *Flemons* and *NewFeet* have a similar scale.

To determine whether *NoFeet* from figure 6 represents a stable structure outside of simulation, we constructed a static prototype. Figure 7 shows this prototype, which consists of wooden dowels, plastic golf balls, and elastic strings held in place with brass hooks. Passive equilibrium due to force distribution is key in tensegrities, and this static prototype shows that *NoFeet* stands in a stable position the same way it does in simulation.

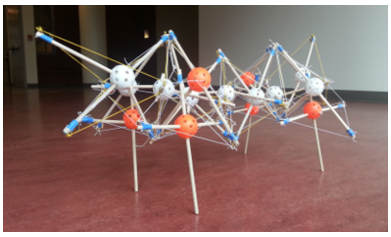

Fig. 7. Static prototype of *NoFeet*.

B. Control

Due to the counter intuitive nature of how these structures move, we found that hand-designing controllers was ineffective, so we turned to machine learning techniques, as originally developed by Mirletz for learning the control for tensegrity spines. Machine learning using CPGs and a neural network for feedback, as discussed in section III, was used to actuate *LongTorso*, *Spirals*, and *NoFeet* from figures 4, 5, and 6 in simulation. Figure 8 shows the results for *LongTorso* from figure 4. As can be seen, only five of the 30,000 controllers achieved a distance greater than 30 cm/min, and only one of these controllers yielded a distance greater than 50 cm/min. Table II shows that genetic evolution more than doubled this distance, to 110.857 cm/min.

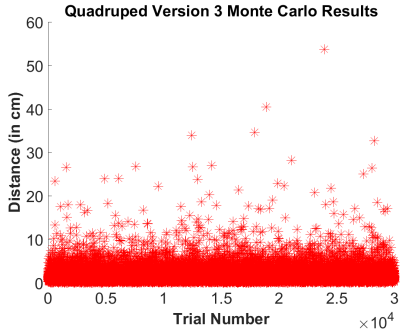

Fig. 8. Distance traveled by *LongTorso* over 30000 Monte Carlo trials.

Figure 9 shows the results of 30,000 Monte Carlo trials for *Spirals*, from figure 5. Although the extra spirals of muscles added to *Spirals* did not improve the farthest distance traveled over 30,000 Monte Carlo trials, the total number of Monte Carlo trials that traveled farther than 30 cm/min increased from 5 to 18, and the number of trials that achieved close to 50 cm/min increased from 1 to 4. Table II shows that evolution yielded a more than 100% improvement with a distance of 130.417 cm/min. This shows that this change in morphology, with the aim of increasing torsion in the spine, improved distance outcomes in CPG control.

NoFeet, from figure 6, showed the best results over both Monte Carlo and evolution. The farthest distance yielded, which was 115.891 cm/min was more than double the farthest distance of *LongTorso* and *Spirals*. As can be seen in figure 10, seven of the trials traveled a distance greater than 100 cm/min, and many more traveled distances greater than 50 cm/min than for *LongTorso* and for *Spirals* from figures 4 and 5. Table II shows that genetic evolution yielded a distance of 228.564 cm/min. These gains from removing the feet show that distance was indeed lost from having feet with too much compliance. The resulting increase in ground reaction force from removing the feet led to increased speed.

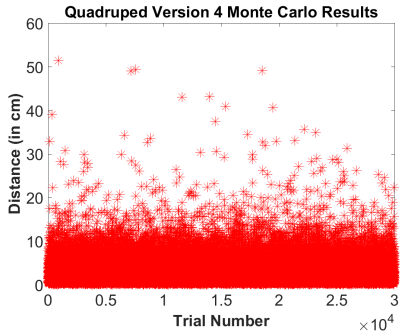

Fig. 9. Distance traveled by *Spirals* over 30000 Monte Carlo trials.

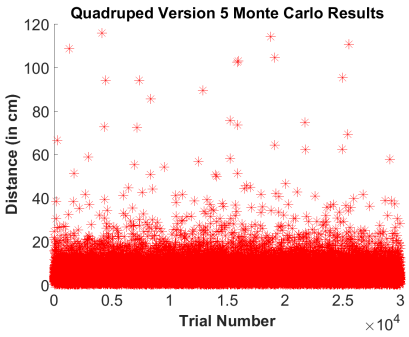

Fig. 10. Distance traveled by *NoFeet* over 30000 Monte Carlo trials.

TABLE II
FARTHEST DISTANCE PER MINUTE FOR EACH MODEL

Model	Monte Carlo	Evolution
LongTorso	53.691 cm/min	110.857 cm/min
Spirals	51.429 cm/min	130.417 cm/min
NoFeet	115.891 cm/min	228.564 cm/min

Figure 11 shows the increase in distance over subsequent generations of evolution. This particular plot comes from the evolution of the best 40 trials from *LongTorso*, shown in figure 4, and for which the Monte Carlo results are shown in figure 8. Note that the total distance increases more quickly over the first 20 generations than it does over the last 40 generations. This shows an example of how the machine learning and control scheme described in section III converges to a near-optimal locomotion gait for a given morphology.

Figure 12 shows the trajectory of the center of mass of *NoFeet*, from figure 6, over one minute. This shows that the simulated robot takes a slightly curved path during travel. While the robot does not yet move quickly, we are still in the early stages of developing the theories of morphological design. The current model of MountainGoat does not yet even have knees, for instance, which would enhance the robot's ability to move over rugged terrain.

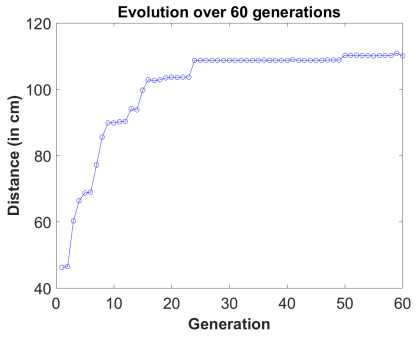

Fig. 11. The distance traveled over 60 generations using control policies dictated by the 40 most successful Monte Carlo trials for *LongTorso*.

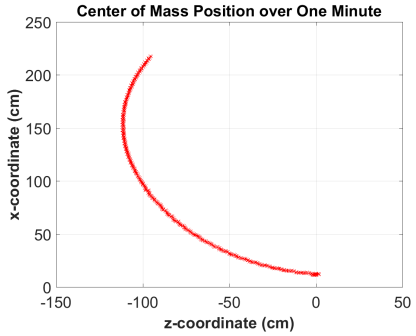

Fig. 12. Trajectory of *NoFeet's* center of mass over a one-minute simulation.

The machine learning results shown in figures 8, 9, and 10 and in table II yield interesting results about the complexities of morphological design of tensegrity structures for locomotion. The passive compliance of the tensegrity quadruped is very valuable, as it allows for nature force distribution and passive terrain adaptation. Yet passive compliance in some cases hinders the effectiveness of locomotion, as can be noted from the differences in the Monte Carlo results for *Spirals* and *NoFeet*, in figures 9, and 10, as well as the farthest distances traveled in table II. More productive motion was gained from reducing compliance in this part of MountainGoat.

The advantage of tensegrity robots is that pretension and stiffness can have different settings in various body parts to enable more productive motion, as shown in table I, where the legs of *LongTorso*, *Spirals*, and *NoFeet* have greater stiffness and pretension settings than the spine does. The

ability for components of the robot to be either compliant or stiff is a unique characteristic of tensegrity robots. But, the morphology of the structure must be designed correctly to be able to provide those points of stiffness, such as lifting the shoulder via the spiral spine muscles added to *Spirals*, from figure 5, which increased the distance traveled after Monte Carlo and genetic evolution. How to design for both passive compliance and active stiffness is an open research topic, for which there is currently no guiding theory.

V. CONCLUSIONS AND FUTURE WORK

Our research explored the coupled aspects of morphological design of a spine-driven tensegrity quadruped, MountainGoat, and evaluation of the resulting CPG controlled locomotion in simulation. Each improvement to structural design increased the distance traveled by the robot. These preliminary results show that we are starting to gain an understanding of the process of whole-body control, where the spine is central to locomotion and how extra support of the shoulders from the spine are necessary in order to lift the legs.

Future work will involve more formal analysis of design metrics and trade-offs, using evolution to optimize MountainGoat's structure in addition to its controller. This will aid in fine tuning aspects of the model such as the optimal number of vertebrae, distance between legs, shape of legs and vertebrae, stiffness and pretension of muscles, and arrangement of muscles. More torsion as and bending the the saggital plane will be added to the spine, to increase torsion to lift legs. Knees and an achilles tendon will be added to the legs, as well as controller optimization to drive motion of the legs, to help with locomotion over rough terrain.

ACKNOWLEDGMENT

The authors thank Brian Mirletz for developing and advising on the learning and control framework, as well as Tom Flemons for his initial quadruped design and inspiration. They also thank Jian Hao Miao, Kevin Le, and Joshua Gier for their work on schematics and construction of the static prototype. Additional thanks goes to members of the NASA Ames Intelligent Robotics Group as well as members of DANSER Lab at UCSC for all their encouragement and support.

REFERENCES

[1] K. Snelson, "Continuous tension, discontinuous compression structures. united states patent 3169611," Feburary 1965.

[2] T. Flemons, "The bones of tensegrity," *http://www.intensiondesigns.com/bones_of_tensegrity*, 2012.

[3] A. L. Xydes, "Simulating ductt and optimizing control for ductt with machine learning," Ph.D. dissertation, UNIVERSITY OF CALIFORNIA, SAN DIEGO, 2015.

[4] A. Iscen, A. Agogino, V. SunSpiral, and K. Tumer, "Robust distributed control of rolling tensegrity robot," in *The Autonomous Robots and Multirobot Systems (ARMS) workshop at AAMAS 2013*, 2013.

[5] A. Agogino, V. SunSpiral, and D. Atkinson, "Super Ball Bot - structures for planetary landing and exploration," *NASA Innovative Advanced Concepts (NIAC) Program, Final Report*, 2013.

[6] B. T. Mirletz, "Adaptive central pattern generators for control of tensegrity spines with many degrees of freedom," Ph.D. dissertation, CASE WESTERN RESERVE UNIVERSITY, 2016.

[7] B. T. Mirletz, P. Bhandal, R. D. Adams, A. K. Agogino, R. D. Quinn, and V. SunSpiral, "Goal-directed cpg-based control for tensegrity spines with many degrees of freedom traversing irregular terrain," *Soft Robotics*, vol. 2, no. 4, pp. 165–176, 2015.

[8] B. T. Mirletz, I.-W. Park, R. D. Quinn, and V. SunSpiral, "Towards bridging the reality gap between tensegrity simulation and robotic hardware," in *Intelligent Robots and Systems (IROS), 2015 IEEE/RSJ International Conference on*. IEEE, 2015, pp. 5357–5363.

[9] B. T. Mirletz, R. D. Quinn, and V. SunSpiral, "Cpgs for adaptive control of spine-like tensegrity structures," in *Proceedings of 2015 International Conference on Robotics and Automation (ICRA2015) Workshop on Central Pattern Generators for Locomotion Control: Pros, Cons & Alternatives*, 2015.

[10] B. Mirletz, I.-W. Park, T. E. Flemons, A. K. Agogino, R. D. Quinn, and V. SunSpiral, "Design and control of modular spine-like tensegrity structures," in *The 6th World Conference of the International Association for Structural Control and Monitoring (6WCSCM)*, 2014.

[11] B. R. Tietz, R. W. Carnahan, R. J. Bachmann, R. D. Quinn, and V. SunSpiral, "Tetraspine: Robust terrain handling on a tensegrity robot using central pattern generators," in *AIM*, 2013, pp. 261–267.

[12] M. Raibert, K. Blankespoor, G. Nelson, R. Playter, and T. Team, "Bigdog, the rough-terrain quadruped robot," in *Proceedings of the 17th World Congress*, vol. 17, no. 1, 2008, pp. 10 822–10 825.

[13] E. Ackerman, "Spot is boston dynamics nimble new quadruped robot," *IEEE Spectrum*, 2015.

[14] J. Degrave, K. Caluwaerts, J. Dambre, and F. Wyffels, "Developing an embodied gait on a compliant quadrupedal robot," in *Intelligent Robots and Systems (IROS), 2015 IEEE/RSJ International Conference on*. IEEE, 2015, pp. 4486–4491.

[15] S. Gracovetsky, "An hypothesis for the role of the spine in human locomotion: a challenge to current thinking," *Journal of biomedical engineering*, vol. 7, no. 3, pp. 205–216, 1985.

[16] Q. Zhao, H. Sumioka, K. Nakajima, X. Yu, and R. Pfeifer, "Spine as an engine: effect of spine morphology on spine-driven quadruped locomotion," *Advanced Robotics*, vol. 28, no. 6, pp. 367–378, 2014.

[17] J. Duperret, G. Kenneally, J. Pusey, and D. Koditschek, "Towards a comparative measure of legged agility," in *Experimental Robotics*. Springer, 2016, pp. 3–16.

[18] C. Paul, J. W. Roberts, H. Lipson, and F. J. V. Cuevas, "Gait production in a tensegrity based robot," in *Advanced Robotics, 2005. ICAR'05. Proceedings., 12th International Conference on*. IEEE, 2005, pp. 216–222.

[19] S. Seok, A. Wang, M. Y. M. Chuah, D. J. Hyun, J. Lee, D. M. Otten, J. H. Lang, and S. Kim, "Design principles for energy-efficient legged locomotion and implementation on the mit cheetah robot," *Mechatronics, IEEE/ASME Transactions on*, vol. 20, no. 3, pp. 1117–1129, 2015.

[20] S. Levin, "The tensegrity-truss as a model for spine mechanics: Biotensegrity," *Journal of Mechanics in Medicine and Biology*, vol. 2, pp. 375–388, 2002.

[21] K. Caluwaerts, J. Despraz, A. Işçen, A. P. Sabelhaus, J. Bruce, B. Schrauwen, and V. SunSpiral, "Design and control of compliant tensegrity robots through simulation and hardware validation," *Journal of The Royal Society Interface*, vol. 11, no. 98, p. 20140520, 2014.

[22] S. Grillner, A. Kozlov, P. Dario, C. Stefanini, A. Menciassi, A. Lansner, and J. H. Kotaleski, "Modeling a vertebrate motor system: pattern generation, steering and control of body orientation," *Progress in brain research*, vol. 165, pp. 221–234, 2007.

[23] O. Orki, A. Ayali, O. Shai, and U. Ben-Hanan, "Modeling of caterpillar crawl using novel tensegrity structures," *Bioinspiration & biomimetics*, vol. 7, no. 4, p. 046006, 2012.

[24] L. Righetti, J. Buchli, and A. J. Ijspeert, "Dynamic hebbian learning in adaptive frequency oscillators," *Physica D: Nonlinear Phenomena*, vol. 216, no. 2, pp. 269–281, 2006.

[25] S. Gay, J. Santos-Victor, and A. Ijspeert, "Learning robot gait stability using neural networks as sensory feedback function for central pattern generators," in *Intelligent Robots and Systems (IROS), 2013 IEEE/RSJ International Conference on*. Ieee, 2013, pp. 194–201.

[26] M. Mulansky and K. Ahnert, "Odeint library," *Scholarpedia*, vol. 9, no. 12, p. 32342, 2014.